ISTANBUL TECHNICAL UNIVERSITY ★ INSTITUTE OF SCIENCE AND TECHNOLOGY

EVALUATION AND COMPARISON OF IMAGE QUALITY FOR INDIRECT FLAT PANELS WITH CsI AND GOS SCINTILLATORS

M.Sc. Thesis by
Erkan AKKUR

Department : Electronics & Communication Engineering

Programme : Biomedical Engineering

June 2011

ISTANBUL TECHNICAL UNIVERSITY ★ INSTITUTE OF SCIENCE AND TECHNOLOGY

EVALUATION AND COMPARISON OF IMAGE QUALITY FOR INDIRECT FLAT PANELS WITH CsI AND GOS SCINTILLATORS

M.Sc. Thesis by
Erkan AKKUR
(504081403)

Date of submission : 06.05.2011
Date of defance examination : 08.06.2011

Supervisor (Chairman) : **Assist. Prof. Dr. Mustafa KAMAŞAK (ITU)**
M. Emin AKSOY M.D., MSc., Phd
Members of the Examining
Committee: **Prof. Dr. Bilge GÜNSEL (ITU)**
Assoc.Prof.Dr. Uluğ BAYAZIT(ITU)
Ayhan ÜÇGÜL M.D.

June 2011

İSTANBUL TEKNİK ÜNİVERSİTESİ ★ FEN BİLİMLERİ ENSTİTÜSÜ

CsI VE GOS SİNTİLATÖRÜNE SAHİP FLAT PANEL SİSTEMLER İÇİN GÖRÜNTÜ KALİTESİNİN KARŞILAŞTIRILMASI VE DEĞERLENDİRİLMESİ

YÜKSEK LİSANS TEZİ
Erkan AKKUR
(504081403)

Tez Danışmanı: Yrd. Doç. Dr. Mustafa KAMAŞAK (İTÜ)
                  Uz. Dr. M. Emin AKSOY,Phd.
Diğer Jüri Üyeleri: Prof.Dr.Bilge GÜNSEL (İTU)
                       Doç.Dr.Uluğ BAYAZIT(İTÜ)
                       Uz.Dr.Ayhan ÜÇGÜL

Haziran 2011

FOREWORD

I would like to express my deep appreciation to my supervisors Assist. Prof. Dr. Mustafa KAMASAK and Dr. Emin AKSOY and for the inspiring support and the opportunities they provided me. It was a great pleasure for me to carry on this thesis under their supervision.

I would also like to thank Prof. Dr. Nadir ARICAN, Dr.Ayhan ÜÇGÜL, Biomed.Eng. Duygu TORUN, Physicist Hüseyin ALACA and Naval Arch. And Marine Eng. Mehmet ACAR for sharing their knowledge.

June 2011   Erkan AKKUR
                                                            Biomedical Engineer

TABLE OF CONTENTS

ABBREVIATIONS

CR	**:**	Computed Radiograph
PSP	**:**	Photostimulable Phosphor
CCD	**:**	Charge-Coupled-Devices
DQE	**:**	Detective Quantum Efficiency
SNR	**:**	Signal to Noise Ratio
TFT	**:**	Thin Film Transistor
CsI	**:**	Cesium Iodide
GOS	**:**	Gadolinium Oxysulfate
CNR	**:**	Contrast to Noise Ratio
MTF	**:**	Modulation Transfer Function
NPS	**:**	Noise Power Spectrum
ROC	**:**	Receiver Operating Characteristic
TOC	**:**	Transparent Optical Ceramic
IQF	**:**	Image Quality Figure
IQFinv	**:**	Inverse Image Quality Figure
SSD	**:**	Source to Detector

x

LIST OF TABLES

LIST OF FIGURES

EVALUATION AND COMPARISON OF IMAGE QUALITY FOR INDIRECT FLAT PANELS WITH CSI AND GOS SCINTILLATORS

SUMMARY

The aim of this study is to compare flat panel detectors with cesium iodide (CsI) or gadolinium oxysulfate (GOS) scintillators. CDRAD 2.0 phantom is used to evaluate how CsI and GOS scintillators affect the image quality in terms of contrast and detail. Nine different flat panel systems (from 6 different manufacturers) are evaluated in this study. Four of these flat panels have CsI scintillators and the remaining 5 have GOS scintillators. For image acqusition, 20 layers of Plexiglas were placed on the top (10 layers) and bottom (10 layers) of the CDRAD 2.0 phantom to simulate a patient. 3 images are taken from each system at each dose level, which were analyzed by the CDRAD 2.0 analyzer software. Four different dose levels (50, 100, 150, and 200 µGys) are investigated. IQFinv is used as the quality metric. IQFinv values of GOS systems have little variance both within the same system and between all systems. On the other hand, CsI systems have higher variance in IQFinv values within the same system and between the systems. In addition, same CsI detectors (same model from the same manufacturer) used in different systems resulted in considerable difference in IQFinv values. CsI systems demonstrate 4-5 times more improvement in IQFinv value with increasing dose levels compared to GOS systems. Finally, IQFinv values of CsI systems are higher than GOS systems with statistically significance (p<0.029).

CsI ve GOS SİNTİLATÖRÜNE SAHİP FLAT PANEL SİSTEMLER İÇİN GÖRÜNTÜ KALİTESİNİN KARŞILAŞTIRILMASI VE DEĞERLENDİRİLMESİ

ÖZET

Bu çalışmada, CsI ve GOS sintilatörüne sahip flat panel sistemler için görüntü kalitesinin karşılaştırılması yapılmıştır. CsI ve GOS sintilatörlerinin kontrast ve detay bakımından görüntü kalitesine nasıl etki ettiğini değerlendirmek için CDRAD 2.0 fantomu kullanılmıştır. Bu çalışmada 6 farklı üreticiden olmak üzere 9 farklı ince panelli sistem değerlendirilmiştir. Bu flat panellerden 4'ü CsI sintilatörüne sahipken, kalan 5 tanesi GOS sintilatörüne sahiptir. Değerlendirmelerde, hasta kalınlığını benzetmek için CDRAD fantomunun altına ve üstüne 10'ar pleksiglas tabakalar konmuştur. Her bir sistem için ayrı dozlarda 3'er görüntü alındı ve bu görüntüler CDRAD 2.0 analiz programı ile analiz edilmiştir. Bu çalışmada, 4 farklı doz değerinde (50,100,150 ve 200 µGy) sistemlerin görüntüler elde edilmiştir. Görüntü kalite metriği olarak IQFinv değeri kullanılmıştır. Aynı sistem ve doz için 3 görüntünün IQFinv değerleri hesaplanıp ve bu değerlerin ortalamaları alınmıştır. CsI ve GOS sistemlerinin istatiksel olarak karşılaştırılması için Mann-Whitney U testi kullanılmıştır.

Bu çalışmada, GOS sistemlerinin IQFinv değerleri aynı detektör içinde ve bütün sistemler arasında küçük bir varyans göstermiştir. CsI sistemlerinin IQFinv değerleri ise aynı sistem içinde ve bütün sistemler arasında GOS sistemlerine göre daha yüksek bir değişinti göstermiştir. Ayrıca, aynı CsI detektörü kullanan (aynı üreticiden aynı model) farklı sistemlerin IQFinv değerlerinde önemli farklar olduğu gözlemlenmiştir. Bunun nedenin, sistemlerin kullandığı farklı görüntü işleme yazılımları ve diğer teknik özellikler olduğu düşünülmektedir. Doz artıkça CsI sistemlerinin IQFinv değerleri GOS sistemlerine nazaran 4-5 kat daha hızlı arttığı belirlenmiştir. Son olarak, CsI sistemleri istatistiksel olarak GOS sistemlerinden daha yüksek IOFinv değerlerine sahip olduğu görülmüştür. (p<0.021).

1.INTRODUCTION

The conventional film/screen systems are still used in the radiology because of the good image quality, high spatial resolution and low costs. However, film/screen systems have certain disadvantages such as narrow dynamic range, high repetition rate, archiving cost and impossibility of image manipulation. During the last decade, the digital detectors are gradually replacing the film/screen systems.

Computed radiography (CR) was the first step in the digitalization of radiology. These systems use photostimulable phosphor imaging plates to replace the conventional film/screen systems. After taking each image, the phosphor plate is carried to scanners, where digital images are formed. CR systems have advantages of digital radiology including the wide dynamic range, digital image storage, reduced repetition and image manipulation. However, CR systems have low X-ray quantum conversion efficiency and low spatial resolution.

After CR, digital detectors were introduced. In these systems, the digital images are formed instantly. First digital detectors used CCD cameras to form digital images of x-ray. These detectors were large and difficult to carry. After CCD-based digital detectors, flat-panel systems are introduced in digital radiology. These systems are based on active matrix thin film transistor (TFT) technology. The flat panel systems have higher detective quantum efficiency (DQE) compared to both film/screen and CR systems. In addition, these systems allow an optimized working procedure due to instant image display and the elimination of the film cassettes.

There are two types flat panel detectors; indirect and direct systems. In indirect systems, a scintillator layer absorbs the incident x-rays and converts them into visible light. The visible light is then converted to electric charges by photodiode array and these charges are read out by a TFT array [3-5]. On the other hand, the direct systems use a photoconductor which converts x-ray photons directly into electrical charges read by TFT array.

Different types of scintillators are used in indirect systems. Most commonly used scintillators are structured cesium iodide (CsI) or unstructured gadolinium oxysulfate (Gd_2O_2S-GOS). Thicker layers of scintillator increase the amount of x-ray conversion to visible light and leading to good absorption efficiency. However, thick layers of scintillators increase the amount of scatter which reduce the resolution. In contrast, thin scintillator layers have lower absorption efficiency but better spatial resolution.

CsI scintillators have parallel and discrete needle structured crystals that are approximately 5-10 μm wide. These needles form a channel to the photodiode layer and allow construction of thicker layers without resolution deterioration. GOS scintillators have unstructured granular phosphor screen that are the same type of phosphor used in the conventional intensifying screens. GOS have a disadvantage about low efficiency at high temperatures. In addition, overall light output is better for CsI scintillator, as compared to GOS.

The aim of this study is to compare flat panel detectors with cesium iodide (CsI) or gadolinium oxysulfate (GOS) scintillators. CDRAD 2.0 phantom is used to evaluate how CsI and GOS scintillators affect the image quality in terms of contrast and detail. Nine different flat panel systems (from 6 different manufacturers) are evaluated in this study. Four of these flat panels have CsI scintillators and the remaining 5 have GOS scintillators. For image acqusition, 20 layers of plexiglass were placed on the top (10 layers) and bottom (10 layers) of the CDRAD 2.0 phantom to simulate solid organs in abdominal imaging. Three images are taken from each system, which were analyzed by the CDRAD 2.0 analyzer software.

The rest of this thesis is organized as follows: The second chapter covers literature review about image quality for direct graphy systems. Third chapter describes the setup and methods used for data acquisition and comparison of flat panel systems with cesium iodide (CsI) or gadolinium oxysulfate (GOS) scintillators. Last chapter contains results and discussion of this thesis.

2. LITERATURE REVIEW

X-rays have been in use for over a century since the report of their discovery by Roentgen (1896). X-rays have been used for both diagnosis and treatment of patients. In diagnostic direct graphy, there are two types of imaging systems: Film and digital technology [1].

2.1 Film/Screen Technologies

The conventional film/screen systems have a cassette which consists of one or two intensifying screens. The film and intensifying screen are together called a film/screen combination. Intensifying screens are thin sheets, or layers, of fluorescent materials. The x-ray energy is absorbed by the intensifying screen material. Then,

x-ray is converted into production of multiple visible photons. The film have double emulsion layer which contain silver halide grain. As the grains exposed to light, a latent image is formed. After exposure, there is a chemical reaction in the emulsion layer. As a result, the silver becomes dark. The greater density of exposed grains in regions of the film have higher optical density and appear dark after film processing. The dark regions correspond to greater x-rays absorption in the screen. The general process is shown in figure 2.1[1-4].

Different types of intensifying screens are used in clinic. The selection of a screen for a specific procedure is usually based on a compromise between the requirements for image detail and patient exposure [3].

The conventional film/screen systems contain double intensifier screens mounted on the double emulsion layers. Systems with double emulsion screens have greater sensitivity. This allows lower patient doses [4].

The conventional film/screen systems are still used in the radiology because of the good image quality, high spatial resolution and low costs. However, film/screen systems have certain disadvantages such as narrow dynamic range, high repetition rate, archiving cost and impossibility of image manipulation.
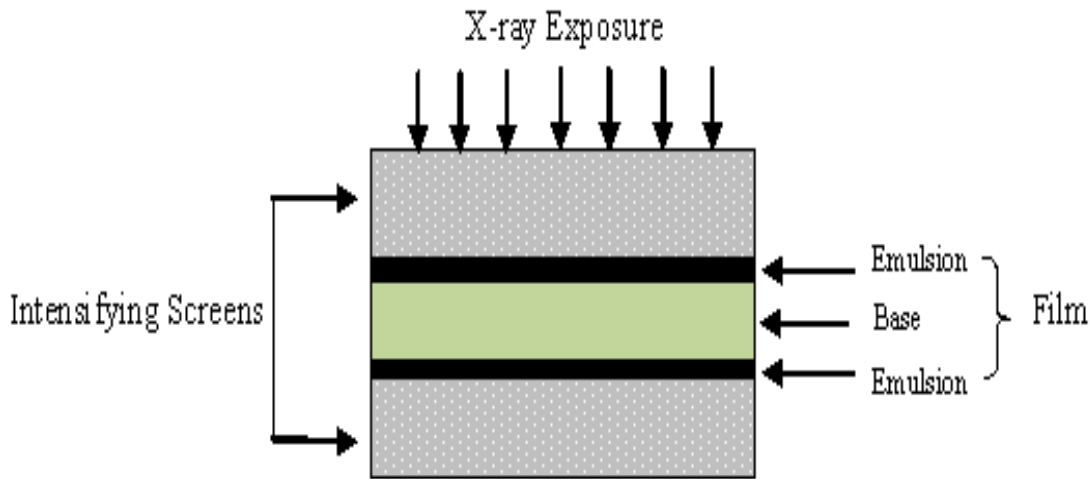
Figure 2.1 : Shematic of conventional screen / film system [1].

2.2 Digital Imaging Systems

During the two past decades, the digital detectors are gradually replacing the film/screen systems. The digital detectors are very flexible in processing and archiving, thus providing a solution to major disadvantages of film/screen systems. Furthermore, digital systems offer greater dynamic range with possible reduction of x-ray exposure to the patient and increase the dose efficiency [5].

The main types of digital detectors are;

- Computed radiography (CR), which uses photostimulable phosphor (PSP) plates,
- Charge-coupled-devices (CCD),
- Indirect and direct flat panel systems.

2.2.1 Computed radiography (CR)

Computed radiography is the first digital system used in radiology. These systems use photostimulable phosphor imaging plates to replace the conventional film/screen systems. The typical phosphor imaging plates consist of europium doped BaFBr and BFI. During the X-ray exposure, the incident radiation excites electrons to higher energy level where some are trapped at meta-stable energy levels (F-centers). The intensities of the incident x-rays are represented by the number trapped electrons in these high energy levels. During the reading out, He-Ne laser is used to release the trapped electrons to drop their original energy state. In this time, light is imaged by a light guide and photomultiplier tube. The light is collected by the photodiodes and

4

converted digitally into an image. The whole readout process takes 30-40 seconds. The general process is shown in figure 2.2 [3-7].
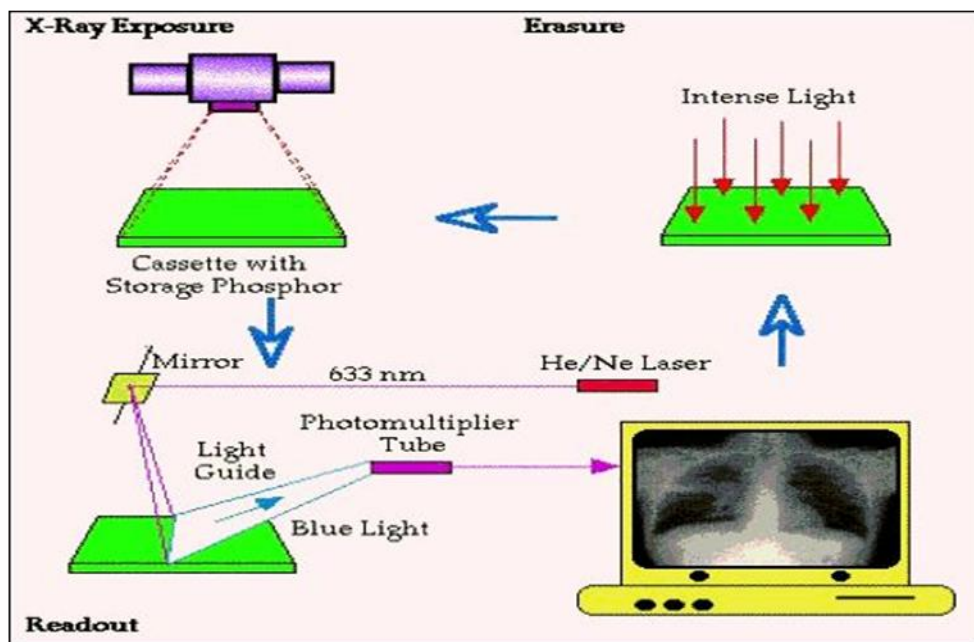

Figure 2.2: Practical implementation of a CR system [4].

The CR systems have wide dynamic range and lower repetition rates. Furthermore, CR systems are cassette-based, so they can easily be integrated into existing radiographic devices. Additionally they are easy to use for bedside examinations and immobile patients. However, CR systems have low X-ray quantum conversion efficiency and low spatial resolution compared to film-screen combinations. Today, CR systems are still used in bedside chest radiography. The dual-reading CR, dual-screen CR and new linear laser diode readout technologies are new technical innovations occurred in CR [3, 4, 5, 7].

2.2.2 Charge-coupled devices (CCD)

Charge coupled devices (CCD) consist of a silicon detector chip, which composes of several million independent pixels. In addition, the detector is combined with an intensifying phosphor screen. This screen emits photons when it is struck by x-rays. The silicon surface of the CCD system is a photosensitive surface for recording images. When the visible photons interact with the pixel, electrons are released and the pixel is built up. Light intensity increases with more electrons produced in a pixel. The general process is shown in figure 2.3 [3-7].
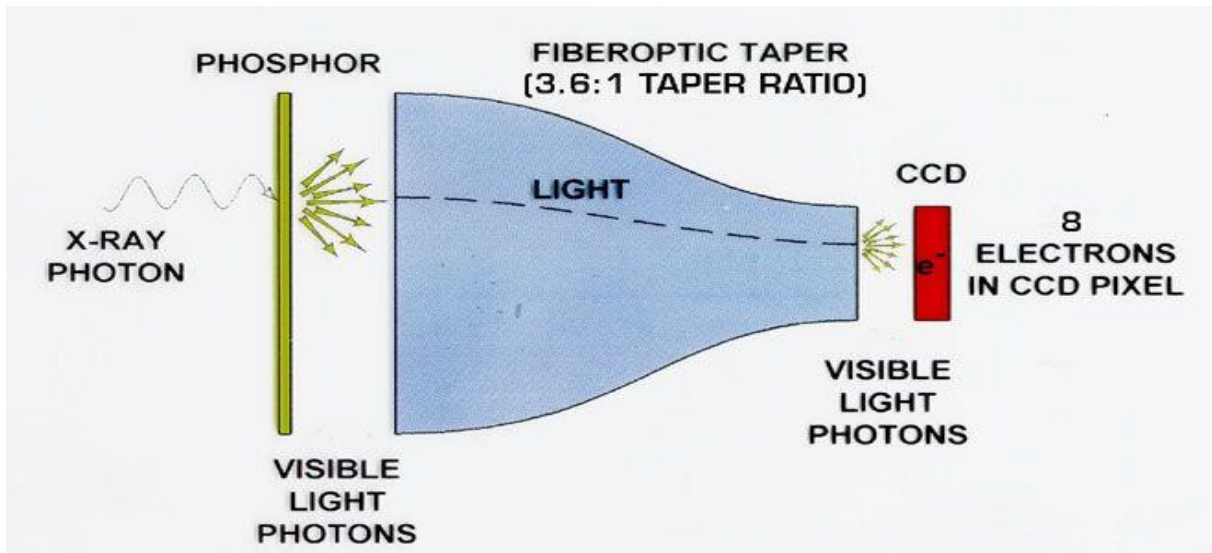
Figure 2.3 : Shematic of a CCD system [4].

CCDs are composed of either a lens-coupled CCD system or slot-scan CCD system. In lens-coupled CCD systems, an array consist of several of CCD ships forms a detector area. Optical lenses are used to reduce the area of the projected visible light image and fit the image to the CCD array. These systems decrease the number of photons reaching CCD (Figure 2.4). As a result, signal to noise ratio (SNR) and detective quantum efficiency (DQE) decrease. Slot –scan CCD systems use a special x-ray tube with a tungsten anode. The patient is scanned with a fan beam of x-rays. The CCD detector arrays collect the emitted light and convert it into electric charges. These systems have low DQE and low SNR (Figure 2.5) [5-7].
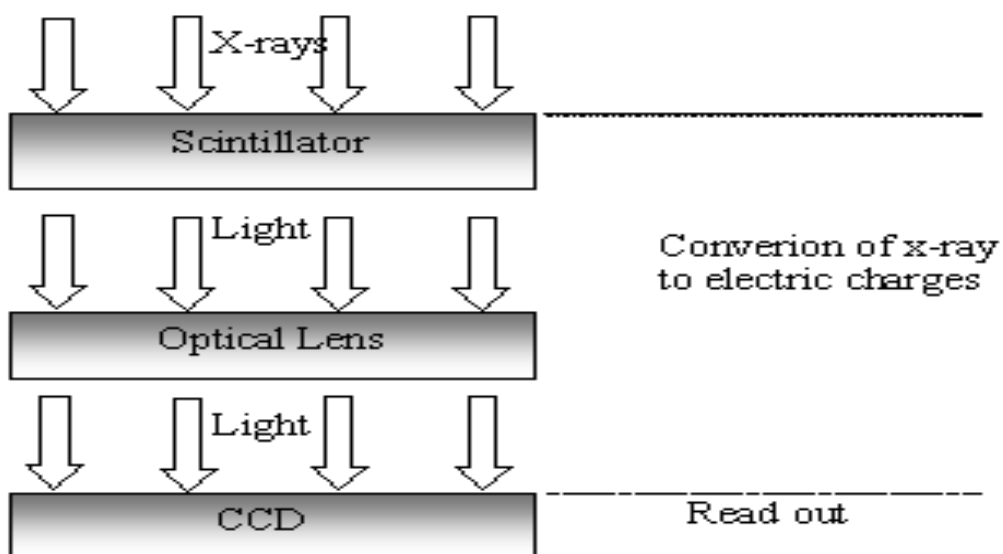
Figure 2.4 : The illustration of lens-coupled CCD systems [5].
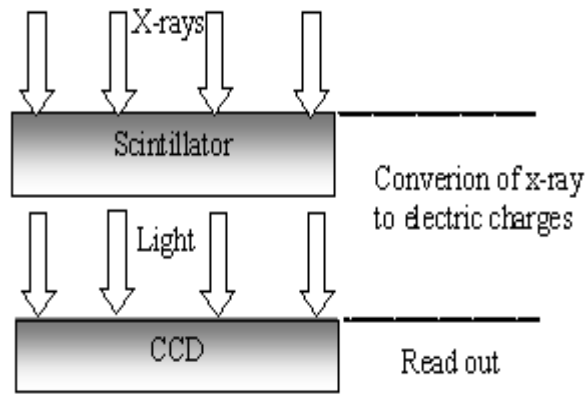
Figure 2.5 : The illustration of lens-coupled CCD systems [5].

2.2.3. Flat panel detectors

Today, flat-panel systems are widely used in digital radiology. These systems are based on active matrix thin film transistor (TFT) technology. The flat panel systems have higher DQE compared to both screen-film and CR systems. In addition, these systems allow an optimized working procedure due to instant image display and the elimination of the film cassettes.

Depending on differentiated X-ray detection principle, the flat panel systems can be classified as either indirect or direct. The direct systems use a photoconductor which converts X-ray photons directly into electrical charges which are read by TFT array. On the other hand, in indirect systems, a scintillator layer absorbs the incident X-rays and converts them into visible light. The visible light is then converted to electric charges by photodiode array and these charges are read out by a TFT array [4-9].

2.2.3.1 Direct flat panel systems

Direct flat panel systems consist of a layer of photoconductor material above a TFT layer. The photoconductor is typically amorphous selenium with a high atomic number. Low atomic number selenium is not ideal as a photoconductor. Before the exposure, an electric field is applied across the photoconductor. When the x-rays are absorbed in the detector, electrons and holes are released. Because of the electric field, the electric charges are directly recorded by the TFT arrays. The general process is shown in figure 2.6. In this way, the problem of light scatter is reduced. Hence, these systems have high intrinsic spatial resolution, which is essential for mammography [4-11].

7
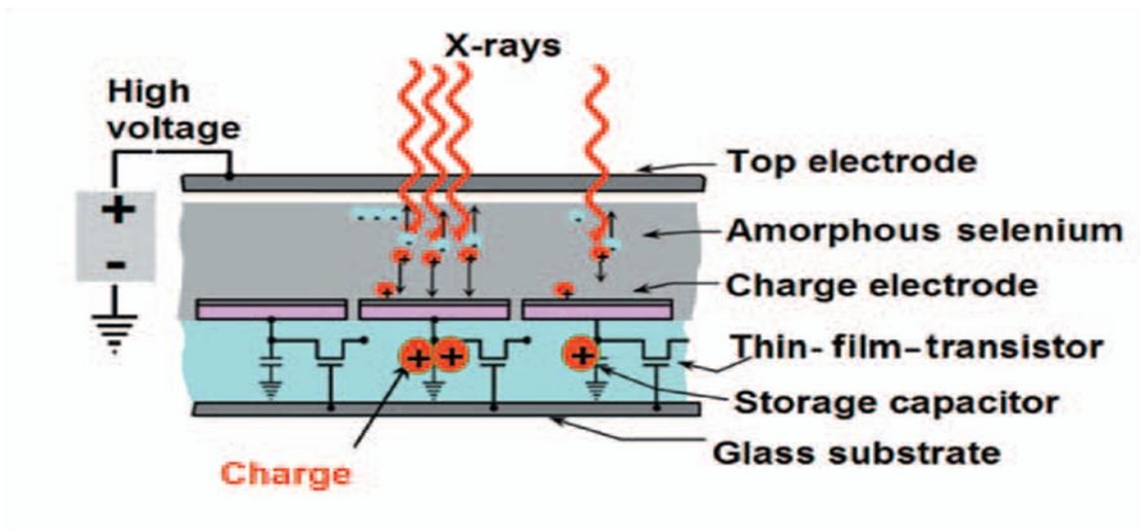
Figure 2.6 : Direct flat panel system. A direct flat panel imager uses a semi-conductor material layered between two electrodes. Local x-ray energy absorption forms the electron pairs. A-high-voltage bias placed between the electrodes separates the charge pairs with little or no lateral spread [6].

2.2.3.2 Indirect flat panel systems

Indirect systems are constructed as a "sandwich" including a scintillator layer, an amorphous silicon photodiode circuitry and a TFT array (Figure 2.7) [5].
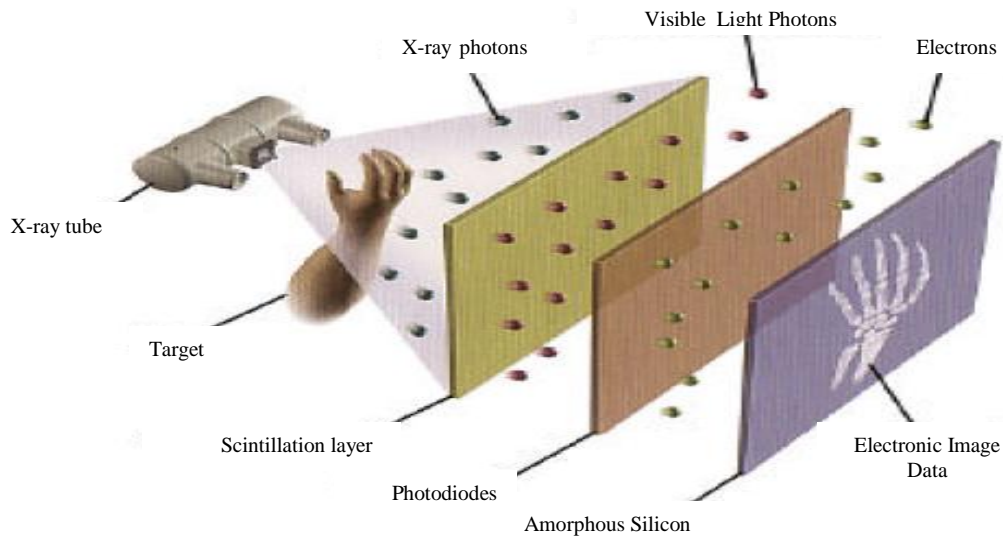
Figure 2.7: Schematic of indirect flat panel systems[11].

As the incident X-rays reach the scintillator, visible light proportional to the incident energy is emitted. Then, visible light photons are converted into electric charge by the photodiode array. These electric charges readout by the TFT array [4-11].

Different types of scintillators are used in indirect systems. Most commonly used scintillators are structured Cesium Iodide (CsI) or unstructured Gadolinium Oxysulfate (Gd_2O_2S - GOS).
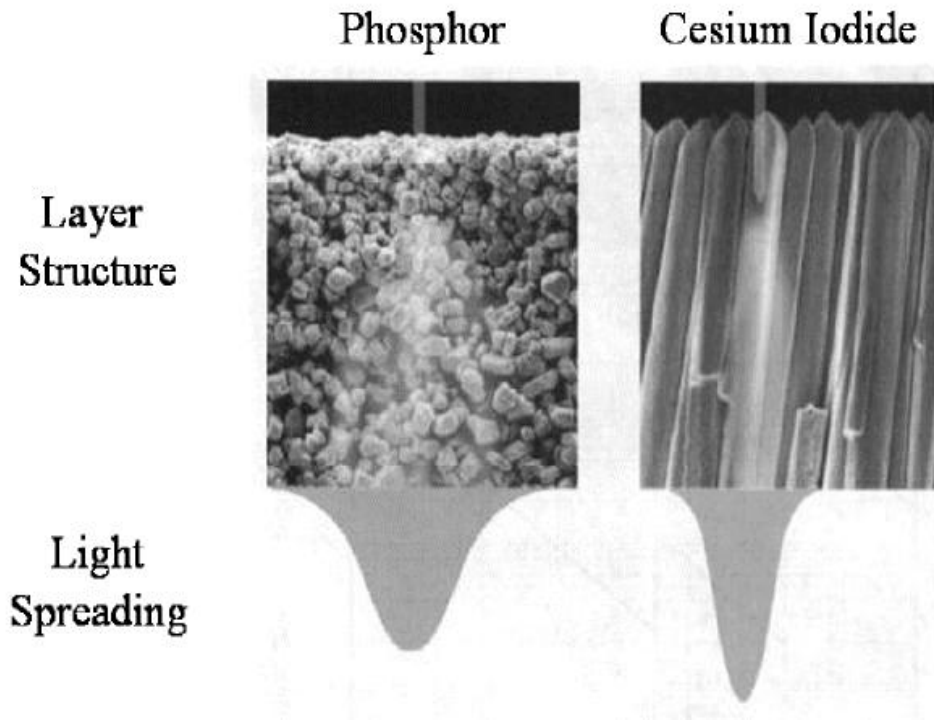
2.2.3.3 Scintillator

Availability of a large area, high light output and high resolving power are very important for scintillators used in the direct systems. Different types of scintillators are used in the indirect systems. Most commonly used scintillators are structured cesium iodide (CsI) or unstructured gadolinium oxysulfate (Gd_2O_2S - GOS) (Figure 2.8) [8].

The GOS scintillators have unstructured granular phosphor screen. It is a well-known technology and its size, thickness and flexibility can be handled easily. In addition, it is cost-effective. This phosphor can come with either a thick or thin screen combination. Thicker layers of scintillator increase the amount of x-ray conversion to visible light and leading to good absorption efficiency. However, thick layers of scintillators increase the amount of scatter which lowers the resolution. In contrast, thin scintillator layers have lower absorption efficiency but better spatial resolution. One of the disadvantages of GOS is marked lowering of efficiency at higher temperatures [8, 9, 12, 13, 14, 15].

The CSI scintillator has multiple advantages. First, it can be readily stored by thermal evaporation at low substrate temperature between 50-250$^{\mathrm{o}}$C. Also, it directly evaporated on a readout pixel array. This avoids the use of optical agents. Therefore, a flat panel system can be produced at a lower cost. Second, CsI scintillators have parallel and discrete needle structured crystals that are approximately 5-10 μm wide. These needles form a channel to the photodiode layer and allow construction of thicker layers without resolution deterioration. Third, the optical photon spectrum emitted CSI matches well with the amorphous silicon material which is usually used to produce a photodiode array. Finally, overall light output is better for CsI scintillator, as compared to GOS [5, 8, 9, 10, 12, 13, 14, 15].

2.2.3.4 The advantages of flat panel system

The most obvious advantages of flat panel systems are their size, reduced dose and resolution. They allow integration of existing Bucky tables or thorax stands. Also,

Figure 2.8: The GOS and the CSI scintillators [8].

image generation with the flat panel system is almost a real time process. Consequently, these systems are highly productive and more patients can be examined in the same amount of time compared to other radiographic devices [4,5].

Another main advantage of these systems over the other systems is that the dose-response curves of flat panel systems are linear over wide exposure range. This is combined with post-processing algorithms, which means that images are better and retakes rates are lower than other systems [4, 5, 6, 7, 8, 10].

2.3. The Imaging Quality Parameters

In medical imaging, a good image quality is very important to assure an accurate diagnosis. Image quality is generally determined by contrast, spatial resolution and noise.

In digital imaging, contrast is described as the contrast-to-noise ratio (CNR). CNR is defined as the signal intensity differences between two image regions A and B with different attenuation divided by the image noise. The equation for contrast to noise ratio is given in equation (2.1);

$$CNR = \frac{(A-B)}{\sigma} \tag{2.1}$$

10

Spatial resolution of an image is defined as the smallest separation between high-contrast objects. Spatial resolution is generally described as visually distinguishable line pairs per mm (lp/mm). In digital radiography, spatial resolution is limited by the minimum pixel size. On the other hand, the smaller pixel size for the systems does not mean higher spatial resolution because scatter of x-ray and light photons within the detector influences spatial resolution [3, 4, 5, 7, 16].

For an effective and detailed information, modulation transfer function (MTF) is used. MTF is used to denote the capacity of the detector to transfer modulation of the input signal at a given spatial frequency to output signal. In digital radiography, objects with different sizes and opacity is shown with different gray-scale values in an image. Therefore, MTF is very important for displaying of contrast and size

[3, 4, 5, 7, 16, 17, 18].

In medical imaging, the noise is present as stochastic component in the image. Different sources of noise can be distinguished in an image. The number of x-ray quanta absorbed by the image receptor is called quantum noise.

The existence of noise influences the contrast detectability of digital systems. The difference between signal and noise can be expressed in the quantity signal to noise ratio (SNR). The SNR can be presented in equation (2.2);

$$\text{SNR} = \frac{N}{\sigma} \tag{2.2}$$

As average number of x-rays in a pixel is denoted by N, the noise in this pixel is expressed σ. The greater number of x-rays that can be detected, the higher is the image SNR [7, 16].

As the imaging systems are compared in terms of signal and noise properties, it is very useful to analyze the noise versus the spatial frequency. The spatial characteristic of noise fluctuations in the image can be determined as a noise power spectrum (NPS) or Wiener Spectrum. The equation for noise power spectrum is given in (2.3).

$$\int \text{NPS(v)dV} = \sigma_{\text{tot}}^2 \tag{2.3}$$

In this equation, σ_{tot} denotes the total image noise [4, 7, 16].

2.4 Assessment of Image Quality

In medical imaging, a correct diagnosis is requires high image quality. Therefore, the the image quality should be measured as accurately as possible. This measurement can be done in several ways and embrace the acquisition part of the digital system or entire system [7].

Physical fundamental characteristics such as spatial resolution, contrast and noise can be analyzed using quantities such as CNR, SNR, MTF and NPS. But, these quantities are abstract measures, thus a direct link with diagnostic image quality is quite difficult to make for these quantities. Furthermore, different methodology (experimental setup and calculations) are used for the measurements of those quantities, particularly for the determination of the MTF [7].

In another method, DQE (Detective quantum efficiency) is used for the assessment of image quality. DQE refers to the efficiency of a detector in converting incident x-ray energy into an image signal. DQE is defined as the ratio of the square of SNR at the detector output to that at the input of the detector as a function of spatial frequency.
DQE is presented in equation (2.4)

$$DQE = \frac{SNR_{out}^2}{SNR_{in}^2} \qquad (2.4)$$

DQE is typically dependent on radiation exposure, spatial frequency, MTF and detector material. In generally, DQE is the best parameter to describe the performance radiographic system. However, the measurement of DQE is very difficult in clinical practice, because the calculation of DQE is very sensitive to small variations in the measurement setup [4, 7, 16].

Previous mentioned image quality parameters concentrate on the performance of detectors. However, these image quality parameters do not include the observer perception in the medical image quality analysis. Indeed, observer perception is very important to show the influence of psychophysical factors in the imaging quality analysis. By using test phantoms, the observer's perception can be tested. The anatomic phantoms are the one of the most of widely used phantoms in the radiology. The anatomic phantoms are designed to imitate the same shaped of hand, chest and pelvis phantom (See figure 2.9). With the using these phantoms, the

observer makes subjective evaluation. In these phantom studies, the observer compares the image with a reference acquisition. Obviously, these phantom studies are the most realistic method for the image evaluation. In addition, they have advantage of being the same images which are being used in clinic without any approximation. However, the natural variability between patients is the major disadvantage. Therefore, the statistical analysis should be used for large numbers of patients [7].

Figure 2.9 :Examples of hand, chest and pelvis anatomic phantoms [7].

For the objective analysis of the image quality in digital radiology, the contrast-detail phantoms have typically been used. These phantoms contain many test objects which are different dimension, form, shape, contrast and size. The contrast-detail phantoms phantom tests the observers' perception. Using this phantom, it is possible to quantify the amount of detail and contrast observed by the observer. The results are given in a contrast-detail curve. In fact, these phantoms allow an image quality assessment of the entire digital imaging system. However, the DQE measurements focus on only the acquisition part. Furthermore, the contrast detail studies provide a more objective and less time consuming, as compared to anatomic phantom studies [4,7 ,19 , 20 ,21 ,22 ,23 ,24 ,25].

Another method of imaging quality is the receiver operating characteristic (ROC). This method based on assessment of an observer of a number of images which contain abnormality. The observer identifies the image as either normal or abnormal which can result in true positive, false positive and false negative responses. After plotting true positive detection fraction, the ROC curve is determined. The ROC technique is the one of the highest accuracy for image quality analysis in clinical setting. On the other hand, the ROC studies are very difficult to set up [4, 7, 16].

2.5 The Studies Comparing Evaluation Of Image Quality For Different x-Ray Systems

There are existing many studies that evaluate the image quality of different radiographic systems. These studies compare different types of radiographic systems against each other using subjective and/or objective methods. Bacher compared the image quality of film/screen, CR, and the indirect and the direct flat panel systems in terms of effective dose in patient and contrast-detail detectability. CDRAD 2.0 and phantom were used in this thesis. The flat panel systems offered high image quality and had a significant dose reduction dose delivered to patients [7].

M. A. Irvine compared the indirect flat panel systems and the CR in paediatric radiography in terms of image quality and radiation dose. In the study, the contrast-detail phantom was used to assess radiographic image quality. According to the studies, the flat panel systems provided lower doses, compared the CR systems. Also, the CR systems performance had similar results, compared the DR systems [4].

There are some studies which compare flat panel, CR and film/screen systems using image quality metrics such as modulation transfer function (MTF), noise power spectrum (NPS), and detective quantum efficiency (DQE) [25, 26].

McEntee et al. compared the amorphous silicon/cesium flat panel systems and the CR. In the study, the CDRAD phantom was used. According to this study, the flat panel systems produced the image quality equal to CR at lower dose. However, the flat panel system had lower doses than CR systems while maintaining equal contrast detail resolution [20].

Another study compared the amorphous silicon and amorphous selenium flat panel systems in terms of image quality and radiation dose. In the study, the CDRAD

phantom was used. In the study, it was found that the amorphous silicon flat panel systems had lower patient dose than the amorphous selenium flat panel systems. In addition, the amorphous silicon flat panel systems and the amorphous selenium flat panel systems produced the similar image quality in the study [24].

Three screens composed of 3 different scintillator materials, namely europium-doped lutetium oxide (Lu_2O_3:Eu31), transparent optical ceramic (TOC), thallium-doped cesium iodide (CsI:Tl; CsI), and terbium-doped gadolinium oxysulfide (Gd2O2S:Tb; GOS) were compared in terms of DQE in another study. According to this study, TOC resulted in the higher DQE than CsI and GOS systems. Also, CsI had higher DQE, compared to GOS systems [12].

Z.F.Lu et al. compared of CR and film/screen combination using a contrast–detail phantom, in terms of patient dose, technique settings, and contrast-detail delectability. This study suggested using a higher kVp setting and additional added filtration would reduce the patient entrance skin dose without compromising the contrast-detail delectability. According to this study, CR had lower patient doses than film/screen systems [23].

3. MATERIALS AND METHODS

3.1.The CDRAD 2.0 Contrast-Detail Phantom Description

The CDRAD 2.0 phantom is constructed in a Plexiglas tablet (26.5x26.5x1 cm^3) (see Fig.3.1).225 cylindrical holes of varying diameters and depths are drilled on this tablet. The depths and diameters of holes are logarithmically sized from to 0.3 to 8.0 mm. The x-ray image will have 225 squares placed on a 15x15 grid. In the rows of the grid, the contrast (the depth of the holes) increases from left to right. In the columns of the grid, the diameter of the holes decreases from top to bottom. In the first 3 rows, there exists a single hole within each square. After the 3rd row, each square has two holes: one in the middle of the square and another in one of the four possible corner of the square. The holes are placed in random corners of the squares and patterns are avoided to mislead the observers [27].
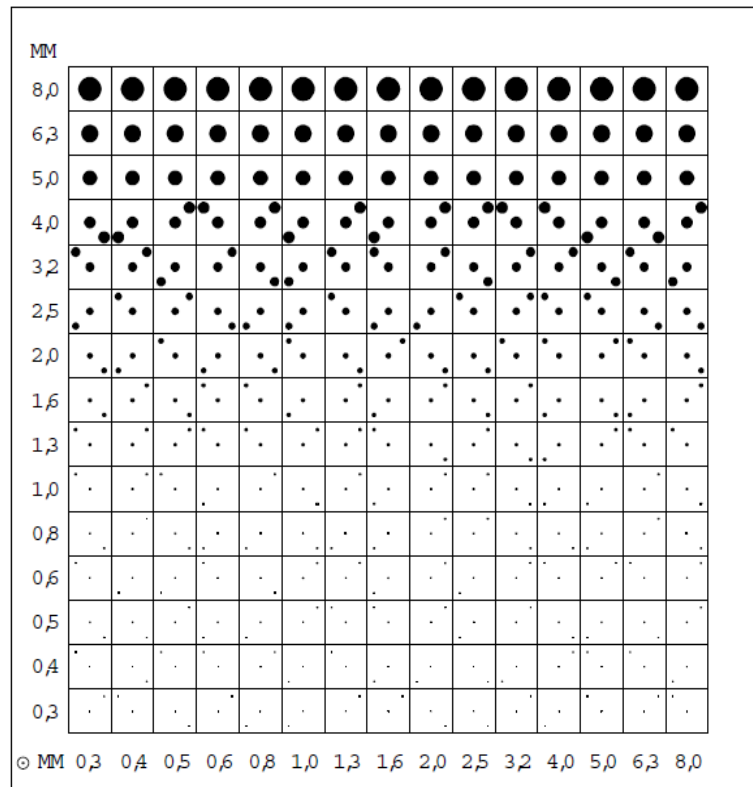
Figure 3.1:Schematic representation of the CDRAD 2.0 phantom.

3.2. CDRAD Analyzer

The CDRAD Analyzer software is developed by the manufacturer of CDRAD phantom. It uses statistical methods to determine whether a certain contrast-detail combination is detected or not. Standard deviation and average pixel value of the image are used in the statistical methods.

The results can be presented in a graph, including the hole-depth and the hole-diameter. The contrast-detail curve is defined the curve through the threshold fields. The image quality can be expressed in a figure by calculation of the ratio of correctly identified hole-positions to the total number of squares [27].

CDRAD Analyzer gives two metrics for image quality. Correct observation ratio is the percentage of the correctly observed squares (the corner of the hole is correctly identified) to the total number of squares. The equation for correct observation ratio is given in (3.1):

$$\text{Correct observation ratio} = \frac{\text{Correct observations}}{\text{Total number of squares}} X 100\% \qquad \textbf{(3.1)}$$

The other metric is called the image quality figure (IQF), which is given in (3.2)

$$\text{IQF} = \sum_{i=1}^{15} C_i \times D(i, th) \qquad \textbf{(3.2)}$$

where D(i,th) denotes the smallest diameter that is correctly observed (shown at each row in Fig. 3.1) and C_i denotes the value in the contrast column (shown under each column in Fig.1) that corresponds to D(i,th). As image quality and IQF are inversely proportional, an inverse image quality figure (IQFinv) is introduced (shown in (3.3)). IQFinv increases with the image quality [27].

$$\text{IQFinv} = \frac{100}{\sum_{i=1}^{15} C_i \times D(i,th)} \qquad \textbf{(3.3)}$$

3.3. Image Acquisition

Images were collected from 9 different flat panel systems produced by 6 differernt vendors. Four of these flat panel detectors had CsI scintillators, and the remaining five had GOS scintillators. To simulate the patient thickness (for abdomen imaging) 10 Plexiglas layers (PMMA) were placed on the top and another 10 PMMA were placed at the bottom (each layer is 26 cm x 26 cm x 1 cm) of the CDRAD 2.0 phantom as shown in Fig. 3.2 and in Fig. 3.3.

Source to detector (SSD) was set as 100 cm and automatic exposure control (AEC) was closed. The generator was set to 80 kVp in manual mode [7, 23, 24, 31]. The mAs values were adjusted to obtain the entrance doses of 50 µGy, 100 µGy, 150 µGy and 200µGy. The achieved entrance dose was measured with dosimeter [Unforms]. For each system, 3 images are taken at a certain entrance dose and recorded in DICOM 3.0 format. The recorded images are analyzed by CDRAD 2.0 Analyzer software. IQFinv values of the 3 images taken from the same system and same entrance value are computed and averaged. The average IQFinv value for each system is plotted at different entrance doses for comparison [7, 28].
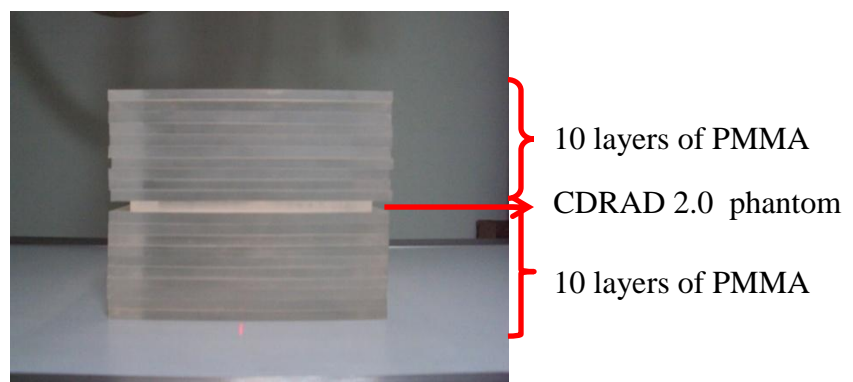
Figure 3.2: Setup for image acquisition.
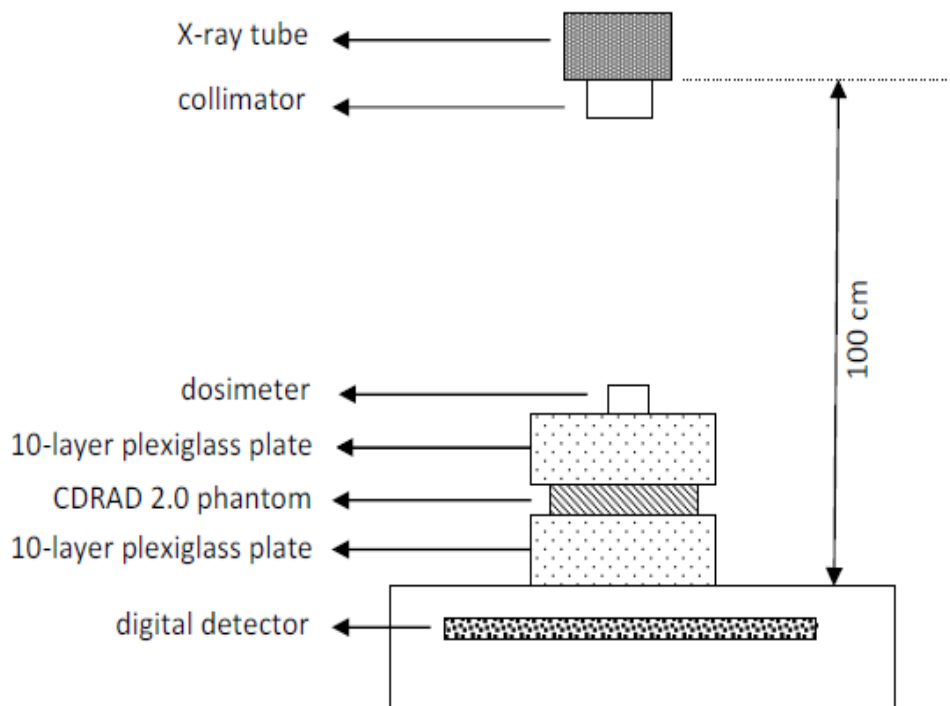
Figure 3.3 Set up for phantom study.

3.4 Data and Statistical Analyzes

Phantom images were collected from 9 flat panel DR systems. Four of these systems had CsI and the remaining five had GOS scintillators. For each system, 12 images (3 images/dose at 4 dose levels) of the phantom were taken. IQFinv values were computed for every image, and these values are averaged for each dose level. Therefore a single IQFinv value is computed for each system and dose level. Systems with GOS and CsI scintillators were compared at each dose level using Mann-Whitney U test [29]. The significance level was determined as 0.05 (α=0.05).

4. RESULTS AND DISCUSSION

4.1 Results

In the Fig. 4.1 and Table 4.1, average IQFinv values corresponding to systems with GOS and CsI scintillators are given for different dose levels. All IQFinv values obtained from different GOS systems at different dose levels are listed in Table 4.2. Similarly, IQFinv values for all CSI systems are given in Table 4.3.

In both systems, the IQFinv values increased with the entrance dose. The relation between the entrance dose (μGy) and IQFinv for GOS and CsI systems are shown in Fig.4.2. Using linear regression, it was shown that the IQFinv value increase faster for the CsI systems compared to the GOS systems.
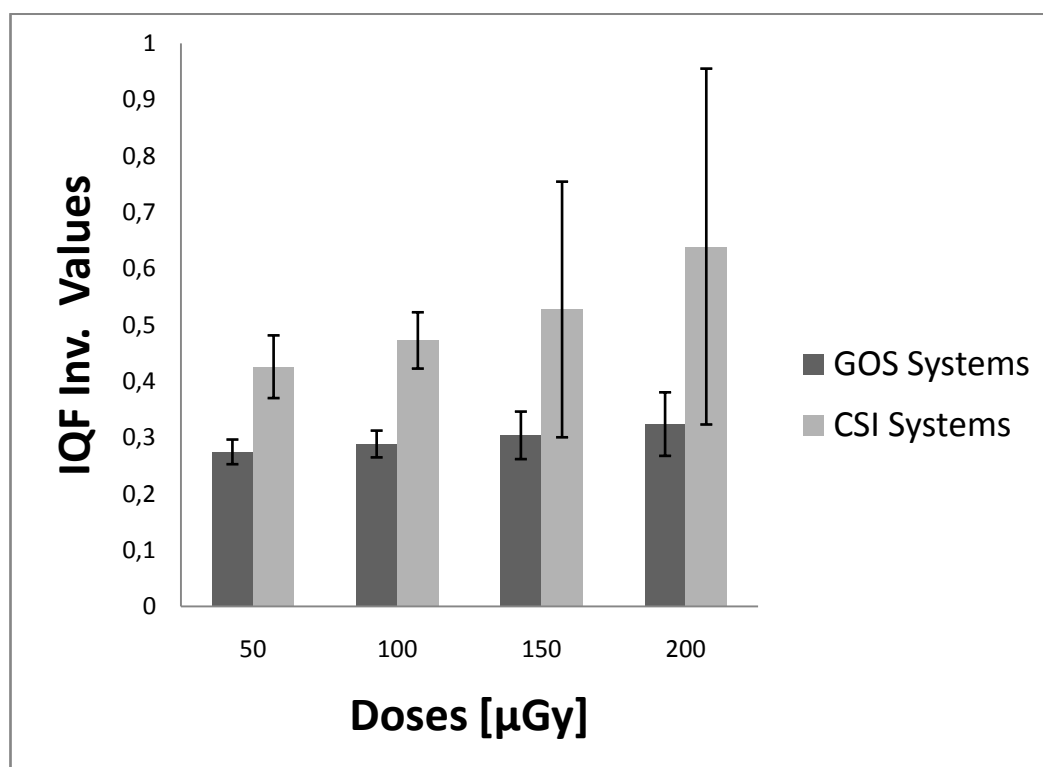
Figure 4.1: Comparison of GOS and CSI Scintillator of flat panel system.

Table 4.1: The mean and the standard deviation of IQFinv values of GOS and CsI systems.

| DOSES (µGy)	GOS Systems		CsI Systems	
	Mean IQFinv	Stdof IQFinv	Mean IQFinv	Stdof IQFinv
50	0,275	0,022	0,425	0,055
100	0,288	0,023	0,472	0,049
150	0,304	0,042	0,527	0,227
200	0,324	0,056	0,639	0,316

Table 4.2: The IQFinv values for GOS systems.

DOSES (µGy)	GOS A			GOS B			GOS C			GOS D			GOS E		
	IQFinv values			IQFinv values			IQFinv values			IQFinv values			IQFinv values		
50	0,32	0,29	0,33	0,26	0,26	0,26	0,28	0,26	0,26	0,26	0,26	0,27	0,29	0,26	0,26
100	0,38	0,32	0,26	0,26	0,26	0,27	0,30	0,32	0,32	0,29	0,26	0,27	0,29	0,26	0,29
150	0,35	0,37	0,39	0,26	0,27	0,26	0,35	0,29	0,32	0,29	0,26	0,29	0,29	0,29	0,27
200	0,40	0,40	0,37	0,26	0,26	0,26	0,40	0,47	0,26	0,30	0,29	0,30	0,30	0,30	0,29

Table 4.3: The IQFinv values for CsI systems.

DOSES (µGy)	CSI A			CSI B			CSI C			CSI D		
	IQFinv values			IQFinv values			IQFinv values			IQFinv values		
50	0,39	0,43	0,26	0,40	0,63	0,43	0,77	0,33	0,26	0,41	0,39	0,41
100	0,65	0,42	0,42	0,66	0,64	0,53	0,45	0,33	0,28	0,45	0,42	0,39
150	0,35	0,39	0,39	0,75	1,28	0,36	0,34	0,32	0,26	0,84	0,79	0,26
200	0,39	0,37	0,37	1,26	1,15	0,81	0,72	0,33	0,26	0,79	0,68	0,54
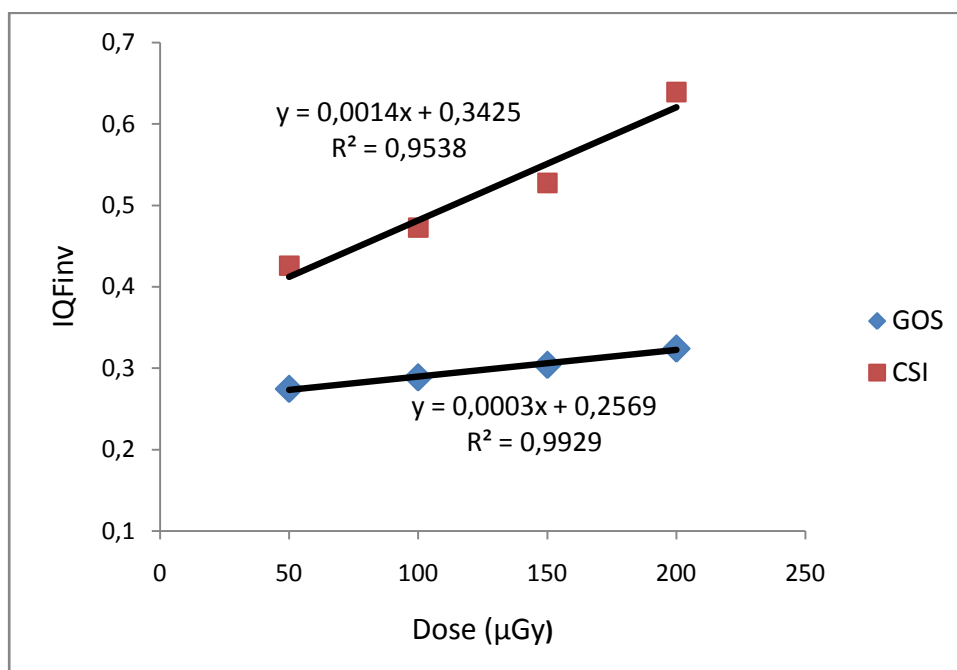
Figure 4.2: The relation between the entrance dose (µGy) and IQFinv for GOS and CsI systems.

4.2 Discussion

In Table 4.1 and Fig. 4.1, mean and standard deviation of averaged IQFinv values among GOS and CsI systems are shown. The mean and standard deviations are computed from IQFinv values given in Table 4.2 and Table 4.3. The coefficient of variation (mean/standard deviation) is small for both GOS and CsI systems at all dose levels except 150 and 200 μGys for CsI systems.

Due to their common structure, detectors with GOS scintillators have similar image quality at different dose levels. From Table 4.2, it can also be observed that IQFinv values of images taken at a specific dose level show little variance within the same system and among all systems. At higher dose levels, the variance of IQFinv values within the same system is still low. On the other hand, the variance of IQFinv values among the systems starts to increase. However, the variance at higher dose levels is still low compared to the mean IQFinv value of the GOS systems.

CsI systems have similar IQFinv values for 50 and 100 μGys. However, their image quality differs at higher dose levels (ie. at 150 and 200 μGys). Table 4.3 gives IQFinv measurements of all CsI systems at different dose levels. From this table, it can be observed that the IQFinv values show more variance compared to GOS systems within the same system at even low dose levels. As the dose increases beyond 150 μGy, the IQFinv variance both within the same system and between all systems is increased to a level approximately 50% of their IQFinv mean value. This indicates that the needle structure of CsI systems shows different performance to tunnel the visible light between image acquisitions at all dose levels. As the dose level increases, the difference between the systems become more substantial.

Some of the DR systems with both GOS and CsI scintillators evaluated in this study use the same flat panel detector (same model from the same manufacturer). However, their IQFinv values are different. This IQFinv difference for the same detector is more noticeable for CsI systems. Different image quality obtained from the same detector may be due to their image processing software and other system specifications.

For both GOS and CsI systems, the IQFinv values increases linearly with dose level. This relation is shown in Fig. 4.2. From this figure, it is observed that CsI systems are approximately 4-5 times more sensitive to dose level compared to GOS systems.

In other words, the image quality of CsI systems improves more than GOS systems with the increasing dose level. This is an expected result as the DQE values of CsI scintillators are higher than GOS scintillators.

The average IQFinv values of CsI and GOS systems are statistically compared. The difference between IQFinv values of these systems is statistically significant ($p < 0.021$). In addition, the average IQFinv values of CsI systems are higher compared to GOS systems with statistical significance ($p < 0.029$).

5. CONCLUSION

In this study, CDRAD 2.0 phantom is used for objective evaluation the contrast-detail characteristics of CsI and GOS scintillators. Nine different flat panel systems were used. Four of these flat panels had CsI scintillators and five had GOS scintillators. For each system, three images for each dose levels were taken. Four different dose levels (50, 100, 150, and 200 μGys) were investigated.

GOS systems show little variance within the same detector and between all systems. On the other hand, CsI systems show higher variance within the same system and between the systems. In addition, same CsI detectors (same model from the same manufacturer) used in different systems resulted in considerable difference in IQFinv values.

CsI systems demonstrate 4-5 times more improvement in IQFinv value with increasing dose levels compared to GOS systems. This result is consistent with the DQE values of CsI and GOS scintillators.

Finally, IQFinv values of CsI systems are higher than GOS systems with statistically significance ($p < 0.029$).

REFERENCES

[1]   **Sprawls, P.**, The Physical Principles of Medical Imaging, *2.end*, [Retrieved 20.06.2011], from http://www.sprawls.org/ppmi2.

[2]   **Webb, A**., 2002. Introduction to Biomedical Imaging, *IEEE Press*, vol. 31(11).

[3]   2007. Practice guideline for digital radiology. in Practice Guidelines and Technical Standarts. Reston Va: *American College of Radiology*, pp.39-72.

[4]   **Irvine, M. A**, 2009. Image Quality and Radiation Dose Comparison of a Computed Radiography System and an Amorphous Silicon Flat Panel System in Paediatric Radiography: A Phantom Study. *MSc thesis,* School of Applied Sciences Science, Engineering and Technology Portfolio RMIT University.

[5]   **Korner, M., Weber, C .H, Wirth, S., Pfeifer, K.J., Reiser, M. F., Treitl, M**., 2007. Advances in Digital Radiography: Physical Principles and System Overview. *Radio graphics*, vol. 27(3), pp.675-686.

[6]   **Seibert, J.A.**, 2009. Digital radiography: the bottom line comparison of CR and DR technology. *Appl. Radiol.* , vol.38, pp.21-28.

[7]   **Bacher, K.,** 2006. Evaluation of image quality and patient radiation dose in digital radiology. *PhD thesis,* Faculty of Medicine and Health Sciences Department of Human Anatomy, Embryology.

[8]   **Kim, H.K., Cunningham, I.A, Yinn, Z, Cho, G.**, 2008. On the Development of Digital Radiography Detectors: A Review. *International Journal of Precision and Manufactuing,* vol 9(4), pp.86-100.

[9]   **Vaidya, P.R.**, 2007. Flat Panel Detectors in Industrial Radiography. *International Workshop on Imaging NDE* , Kalpakkam, Chennai, India.

[10]   **URL 1** <http://www.eradiography.net/cr/dr/Digital Radiography Introduction Kodak.pdf > accessed at 20.06.2010.

[11]   **URL 2** < http://varian.com/media/xray/products/FlatPanelImaging/11.11.04/pdf> accessed at 20.06.2010.

[12] **Cha, B.K., Shin, J.H., Kim, J. Y., Jeon, H., Bae, J.H., Lee, C.-H., Chang, S., Kim, H., Kim, B.-J., and Cho.,G,** 2008. Fabrication and Comparison Gd$_2$O$_2$S(Tb) and CsI(TI), films for X-ray Imaging Detector Application. *IEEE Nuclear Science Symposium Conference Record.*

[13] **Farman, T.T, Vandre, R.H., Pajak, J.C., Miller, S.R., Lempicki, A., Farman, G.,** 2006. Effects of scintillator on the detective quantum efficiency (DQE) of a imaging system. *Oral and Maxillofacial Radiology*, vol (101), pp.219-223.

[14] **Knüpfer, W., Hell, E. and Mattern, D.**, 1999. Novel X-Ray Detectors for Medical Imaging. *Nuclear Physics*, pp. 610-615.

[15] **Nikl, M.**, 2006. Scintillation detectors for x-rays. *Measurement Science and Technology,* vol(17), pp. 37-54.

[16] **Dobbins III, J.T**., 2000. Metrics for Measuring Image Quality. *WA: SPIE Press,* In: Beutel J, Kundel HL, Van Metter RL, eds. Handbook of medical imaging. 1 ed. Bellingham, pp.161-222.

[17] **Floyd, Jr., Warp, R.J, Dobbins III, J.T, Hotas, H.G.C., Baydush, A.H, Vargas-Voracek, R., Ravin, C.E**., 2001. Imaging Characteristics of an Amorphous Silicon Flat-Panel Detector for Digital Chest Radiography. *Medical Physics, Radiology,* vol.218, pp.683-688.

[18] **Wang, X., Van Metter, R.L, Foos, D.H., and Steklenski, D.,** 2006. Comprehensive and Automated Image Quality Performance Measurement of Computed Systems. Health Imaging Research Laboratory, Eastman Kodak Company.

[19] **Lyra, M.E., Kordolaimi, S.D., and Salvara, A-L.N**., 2010. Presentation of Digital Radiographic Systems and the Quality Control Procedures that Currently Followed by Various Organizations Worldwide", *Recent Patents on Medical Imaging*, vol. 2, pp.5-21.

[20] **McEntee, M., Frawley, H., Brennan, P.C**, 2007. A low comparison of low contrast performance for amorphous Silicon/cesium iodide directradiography with a computed radiography: A contrast detail phantom study. *Radiology*, vol. 13, pp.89-94.

[21] **Precht, H., Gerke, O.,** Denmark. DR system: How to find the best hardware and software to achieve minimum dose and optimal image quality. *RC 1414 - Paediatric imaging,* [Retrieved 20.06.2010], from http://www.ucl.dk/media/How_to_find_the_best_hardware_and_software_to.pdf.

[22] **Chotas, H.G. , Ravin, C.E**., 2001. Digital Chest Radiography with a Solid-state Flat- Panel X-ray Detector: Contrast-Detail Evaluation with Processed Images Printed on Film Hard Copy. *USA Radiology*, vol.218, pp.679–68.

[23] **Lu, Z.F., Nickoloff, E.L., So, J.C., and Dutta, A.K.,** 2003. Comparison of the computed radiology and film/screen combination using a contrast detail phantom. *Journal of Applied Clinical Medical Physics*, vol. 4(1), pp.91-98.

[24] **Bacher, K., Smeets, P., Vereecken, L. An De Hauwere, Duyck, P., R.De Man, Verstraete, K. and Thierens, H.,** 2006. Image Quality and Radiation Dose on Digital Chest Imaging: Comparison of Amorphous Silicon and Amorphous Selenium Flat-Panel Systems. *Chest Imaging, AJR:187,* pp.630-637.

[25] **Liu, X., and Shaw, C.C**., 2004. *a*-Si:H/CsI(Tl) flat-panel versus computed radiography for chest imaging applications: image quality metrics measurement, vol.31(1), *Med. Phys,* pp.98-111.

[26] **Samei, E**., 2003. Performance of Digital Radiographic Detectors: Factors Affecting Sharpness and Noise. Advances in Digital Radiography: *RSNA Categorical Course in Diagnostic Radiology Physics*; pp. 49–61.

[27] 2010. Manuals CDRAD 2.0 Phantom & Analyzer Software version, Artinis Medical System.

[28] Y11-Y17-DR Digital Radiography Image Quality. Diagnostic Accrediation Program,Vancouver, Bristish Columbia, [Retrieved 20.06.2010], from http://www.dap.org./CmsFiles/File/SafetyCodeHC35.

[29] **Nachar, N**., 2008. The Mann-Whitney U: A test for assessing whether two independent sample come from the same distribution. *Tutorials in Quantitative Methods for Psychology*, vol 4(1), pp.13-20.

CURRICULUM VITAE

Candidate's full name: Erkan AKKUR

Place and date of Birth: Kayseri-23.05.1984

Universities and Colleges attended:

MSc: Istanbul Technical University, Biomedical Engineering

BSc: Baskent University, Biomedical Engineering

High School: Nermin Mehmet Cekic High School